Applied Surface Science 475 (2019) 559–564

Contents lists available at ScienceDirect

Applied Surface Science

journal homepage: www.elsevier.com/locate/apsusc

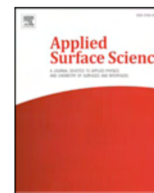

Full Length Article

Surface-enhanced Raman scattering in graphene deposited on $Al_xGa_{1-x}N$/GaN axial heterostructure nanowires

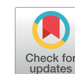

Jakub Kierdaszuk[a,*], Mateusz Tokarczyk[a], Krzysztof M. Czajkowski[a], Rafał Bożek[a], Aleksandra Krajewska[b,c], Aleksandra Przewłoka[b], Wawrzyniec Kaszub[b], Marta Sobanska[d], Zbigniew R. Zytkiewicz[d], Grzegorz Kowalski[a], Tomasz J. Antosiewicz[a], Maria Kamińska[a], Andrzej Wysmołek[a], Aneta Drabińska[a]

[a] *Faculty of Physics, University of Warsaw, Pasteura 5, Warsaw, Poland*
[b] *Institute of Electronic Materials Technology, Wólczyńska 133, Warsaw, Poland*
[c] *Institute of Optoelectronics, Military University of Technology, Kaliskiego 2, Warsaw, Poland*
[d] *Institute of Physics, Polish Academy of Sciences, Lotników 32/46, Warsaw, Poland*

ARTICLE INFO

Keywords:
Graphene
Nanowires
Gallium nitride
Polarization
Raman spectroscopy
Electroreflectance
Carrier concentration
KPFM

ABSTRACT

The surface-enhanced Raman scattering in graphene deposited on $Al_xGa_{1-x}N$/GaN axial heterostructure nanowires was investigated. It was found that the intensity of graphene Raman spectra is not correlated with aluminium content. Analysis of graphene Raman band parameters, Kelvin probe force microscopy, and electroreflectance showed a screening of polarisation charges. Theoretical calculations demonstrated that plasmon resonance in graphene is far beyond the Raman spectral range. This excludes the presence of an electromagnetic mechanism of surface-enhanced Raman scattering, hence suggesting a chemical mechanism of enhancement.

1. Introduction

Studies of graphene deposited on vertically aligned gallium nitride nanowires (GaN NWs) are interesting because of possible applications (such as in photovoltaics, photodetectors, light emitting diodes, or water splitting), and owing to the presence of surface-enhanced Raman scattering in graphene [1–7]. The intensity of Raman bands has been found to be more than one order of magnitude higher in graphene on NWs than in graphene deposited on GaN epilayer. This effect is not related to an enhancement observed in free-standing graphene because it is not present in graphene on NWs with unequal heights [8,9]. Our previous results have excluded light interference in NW layers being responsible for this enhancement [9]. However, they have not explained which of the two mechanisms of enhancement (electromagnetic or chemical) dominates. The chemical mechanism assumes that Raman spectra enhancement is caused by the charge-transfer resulting from chemical bonding at the GaN/graphene interface. The surface-enhanced Raman scattering (SERS) effect in N719 black dye adsorbed on GaN bundles of nanowires has been recently observed [10]. It was related to the chemical mechanism where charge transfer between the GaN valence band and the LUMO level of the dye play a major role. However, the possibility of electromagnetic enhancement was not discussed. The electromagnetic mechanism is related to the formation of surface plasmons in the graphene due to the existence of polarisation charges on top of the nanowires [11]. AlGaN is a wide bandgap semiconductor with a wurtzite structure. Due to the spontaneous and piezoelectric polarisation along the c-axis, which in this case is perpendicular to the surface, a high concentration of polarisation charges is present on its surface [12,13]. Polarisation charges are usually screened by free carriers. However, recent works have indicated that the NW structure reduces the free carrier screening effect, which enables the creation of piezo-generators integrating a vertical array of GaN NWs [14]. Total electric polarisation in AlGaN consists of spontaneous polarisation (P_{SP}) and of piezoelectric polarisation (P_{PE}). Both polarisation components increase with aluminium content (x) in $Al_xGa_{1-x}N$ [12]. However, the detailed discussion of actual polarisation charge density on the top surface of NW needs to be extended by calculating the exact value of piezoelectric polarisation using the lattice parameters, which can be obtained from X-ray diffraction. An additional technique that can provide information about the electric field present in the structure

* Corresponding author.
E-mail address: jakub.kierdaszuk@fuw.edu.pl (J. Kierdaszuk).

https://doi.org/10.1016/j.apsusc.2019.01.040
Received 24 September 2018; Received in revised form 2 January 2019; Accepted 4 January 2019
Available online 05 January 2019
0169-4332/ © 2019 Elsevier B.V. All rights reserved.

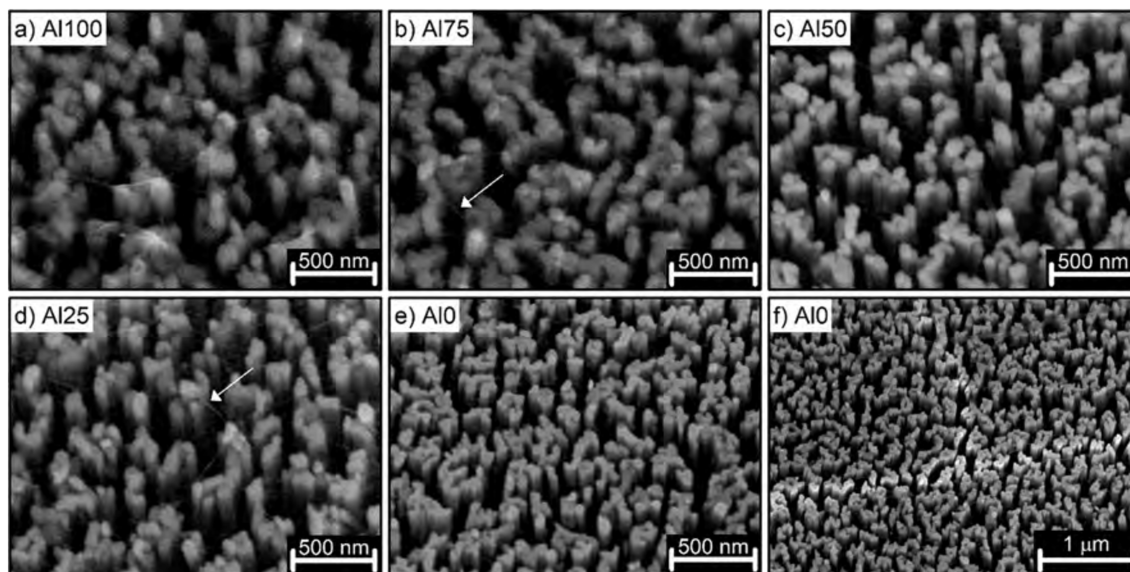

Fig. 1. SEM image of graphene deposited on GaN NWs with different aluminium contents under a 20° tilt. The grey colour indicates NWs covered by graphene, while black corresponds to graphene areas hanging in-between nanowires. For the Al0 sample, an additional image with smaller magnification is presented (f) to show NWs which were not covered by graphene (white colour). Two examples of graphene wrinkles are indicated with white arrows.

is electroreflectance spectroscopy [15,16]. Observation of Franz-Keldysh oscillations in electroreflectance spectra provides direct evidence of the presence of electric fields caused by polarisation charges [17]. On the other hand, energies and widths of the graphene G and 2D bands depend on both carrier concentration and graphene strain [18,19]. Raman spectroscopy and atomic force microscopy of graphene deposited on nanopillars with equal height show the presence of strain, which depends on the distances between the nearest pillars [20,21]. Moreover, measurements of graphene top-gated transistors show the dependence between carrier concentration and various Raman band parameters [18]. Previous Raman measurements of graphene on NWs show the presence of nanogating caused by interaction with these NWs [9]. Thus, Raman micromapping allows the tracing of how AlGaN NWs locally gate graphene and change its carrier concentration and strain [9]. Furthermore, Kelvin probe force microscopy (KPFM) was applied to measure the topography of graphene deposited on $Al_xGa_{1-x}N$ NWs and the distribution of potential on the graphene surface. The potential in graphene is proportional to the carrier concentration [22]. Therefore, KPFM measurements enable the investigation of the effects of different NW surfaces on the carrier concentration in graphene and, consequently, their nanogating with better resolution than using Raman spectroscopy [9]. Thus, studies of graphene deposited on $Al_xGa_{1-x}N$ NWs with different compositions should provide an insight on how electric field induced in NWs influences the SERS effect in graphene. Further, it should be recognised which enhancement mechanism is dominant.

2. Materials and methods

GaN NWs were grown by plasma assisted molecular beam epitaxy on Si(1 1 1) substrate under N-rich conditions without the use of any catalyst [23]. After a growth of 900 nm of GaN NWs, the Al source was opened and 100 nm of $Al_xGa_{1-x}N$ were grown. The crystallographic orientation of NWs was (0 0 0 −1). During our measurements, several samples with x content varying from 0 to 1 were studied (named from Al0 to Al100, respectively). Nanowire diameters of all samples were approximately 40 nm and the nanowire density was approximately 140 μm^{-2}. Graphene was grown by chemical vapour deposition on Cu foil by methane precursor [24]. A polymer frame was used to transfer graphene onto the NW substrates [25]. Scanning electron microscopy (SEM) measurements were performed on a microscope integrated with a Helios Nanolab 600 Focus Ion Beam. It was equipped with a secondary electron detector at an electron beam voltage of 5 kV. A Phillips X-pert diffractometer equipped with a Cu sealed tube X-ray source, a four bounce Ge (2 2 0) Bartels monochromator, and a channel-cut Ge (2 2 0) analyser were used for high-resolution X-ray diffraction (HRXRD) measurements. Electroreflectance spectroscopy relies on the measurement of reflectivity during external modulation of the electric field in the structure. In our case, the AC voltage was applied between the graphene and the Si substrate, ensuring the modulation of the electric field in the NWs. The sample was illuminated by monochromatic light and the reflected light was focused onto a silicon diode. The DC and AC signals were measured by a voltmeter and a lock-in amplifier, respectively. A 75 W Xe lamp was used as a light source. Raman measurements were performed by a T64000 Horiba Jobin-Yvon spectrometer with a 532 nm excitation Nd:YAG laser. Raman micromapping for each sample was performed on an area of 9 μm^2 with 100 nm steps, using a 100 x microscope objective with a spatial resolution of approximately 300 nm. KPFM measurements were performed using Digital Instruments Multimode Atomic Force Microscope with a needle of 50 nm in diameter, capable of measuring the electric potential of the specimen. In KPFM measurements, due to the inability to determine the reference potential, values of the measured potential are arbitrary; however, their values and local variations can be compared between the investigated samples.

3. Experimental results

SEM measurements in lower magnification (Fig. 1f) show that the NWs not covered with graphene can be clearly distinguished from those covered by graphene and that the graphene edges are clearly visible. Roughness of graphene on the NWs is low in all investigated samples (Fig. 1). Small wrinkles are caused by an expansion of graphene hanging between the nearest NWs. SEM also confirmed a similar value of NW heights and density distribution on the surface of all investigated samples. HRXRD measurements show peaks related to symmetric 002 and asymmetric 105 GaN and $Al_xGa_{1-x}N$ reflections (Fig. 2a and b). In addition, the asymmetric broadening on the right side of a GaN peak (marked as A) can be observed. This broadening may be caused by the core/shell effect occurring in the axial-heterostructure NWs reported by

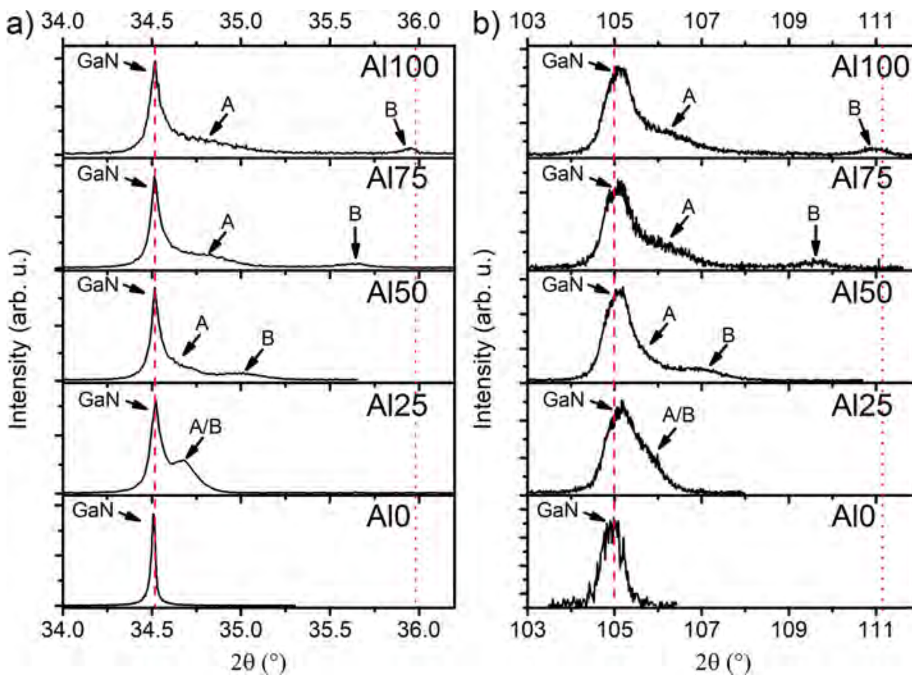

Fig. 2. HRXRD 2θ/ω scans results of: (a) symmetric 002 reflection, (b) asymmetric 105 reflection for all five NW substrates. GaN A and B peaks are indicated; A is the peak from the core-shell with non-nominal value of Al content and B is the peak from the $Al_xGa_{1-x}N$ part of the NWs. Dash and dot lines show nominal angular positions for bulk GaN and AlN crystals, respectively.

Table 1
Values of lattice constants (ε_c, ε_a) for AlGaN and GaN (for Al0 sample), strain in the top layer obtained from HRXRD measurements, calculated values of piezoelectric and spontaneous polarisation (P_{PE}, P_{SP}), and concentration of polarisation charge (n_s) present on $Al_xGa_{1-x}N$ NWs top surface.

X	0	0.25	0.50	0.75	1
c_{AlGaN} (Å)	5.185	5.162	5.125	5.031	4.985
a_{AlGaN} (Å)	3.189	3.181	3.172	3.143	3.127
ε_c (%)	0	0.54	0.82	−0.03	0.06
ε_a (%)	0	0.35	0.68	0.38	0.48
P_{PE} (Cm^{-2})	0	0.001	0.002	−0.005	−0.005
P_{SP} (Cm^{-2})	−0.029	−0.042	−0.055	−0.068	−0.081
n_s (cm^{-2})	$1.8{\cdot}10^{13}$	$2.5{\cdot}10^{13}$	$3.3{\cdot}10^{13}$	$4.5{\cdot}10^{13}$	$5.4{\cdot}10^{13}$

other authors [26–28]. The shell part is strained and has non nominal aluminium content. Its thickness does not exceed 10 nm [27,28]. However, the presence of the shell does not affect the value of aluminium content in AlGaN caps, which was confirmed by the energy-dispersive X-ray spectroscopy studies [28]. Due to the strain, peaks positions differ from the literature values of unstrained GaN and AlGaN [12]. Values of calculated relative strain (ε_c, ε_a) are presented in Table 1 (for calculations $c_{GaN} = 5.185$ Å and $a_{GaN} = 3.189$ Å, GaN lattice constants were used, which were obtained from the HRXRD measurements of the Al0 sample). Spontaneous polarisation in AlGaN can be calculated using the following formula:[12]

$$P_{SP} = -0.052x - 0.029. \tag{1}$$

where x is the aluminium content. The piezoelectric polarisation P_{PE} depends both on x and on strain (ε): [12]

$$P_{PE}(x) = (0.73 + 0.73x)\varepsilon_a + 2(-0.11x - 0.49)\varepsilon_c. \tag{2}$$

The calculated value of P_{PE} in the case of our samples was much smaller than P_{SP} (Table 1), and no explicit correlation between P_{PE} and x was observed.

The total polarisation is the sum of spontaneous and piezoelectric contributions. Non-zero polarisation in AlGaN NWs results in the presence of positive polarisation charge on top of the NWs, with a sheet polarisation charge concentration (n_s) equal to:

$$n_s = \frac{|P_{SP} + P_{PE}|}{e}. \tag{3}$$

In case of our samples, n_s increased with x and varied from 1.8×10^{13} cm^{-2} for the Al0 sample to 5.4×10^{13} cm^{-2} for the Al100 sample (Table 1).

Direct verification of the polarisation charge presence can be performed by the electroreflectance measurements presented in Fig. 3. Due to the spectral range, this technique was only available for samples with the lowest Al content (below 20%). The electroreflectance signal shape depends on the strength of the electric field present in the structure. In the low-field limit, when the energy of the accelerated particle is smaller than the energy broadening, third-derivative line shapes appear. In practice, for GaN heterostructures at room temperatures, this limit is reached if the electric field is lower than 20 kV/cm. If the energy of the accelerated particle is larger than the broadening energy, it is possible to observe the very characteristic Franz-Keldysh oscillations for energies larger than the energy band gap of the material. The period of these oscillations is proportional to the electric field and the amplitude

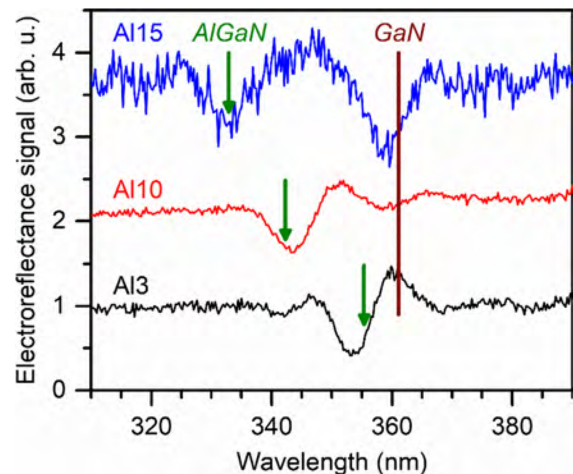

Fig. 3. Electroreflectance spectra of the investigated samples. Wavelength values corresponding to the energy gap of the AlGaN caps are indicated with green arrows, while the brown vertical line indicates the energy gap of GaN.

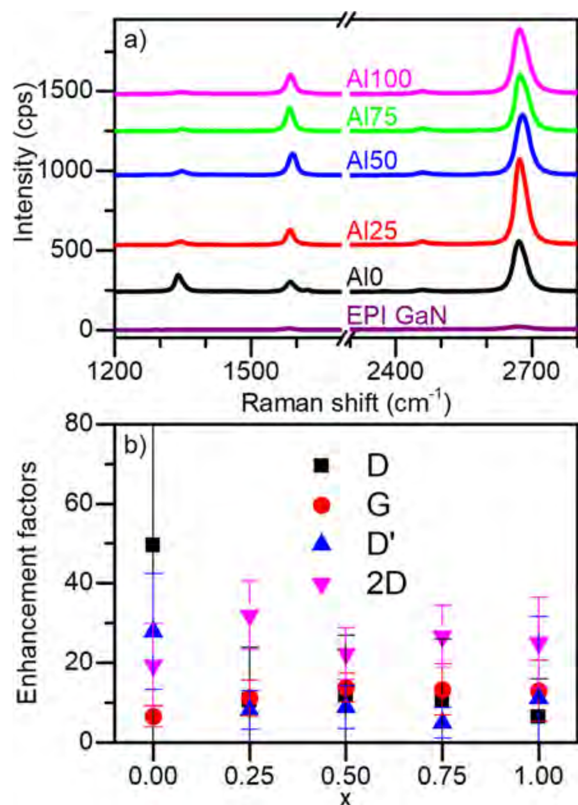

Fig. 4. (a) Raman spectra of investigated samples and reference samples of graphene on GaN epilayer, (b) enhancement factors for each Raman bands.

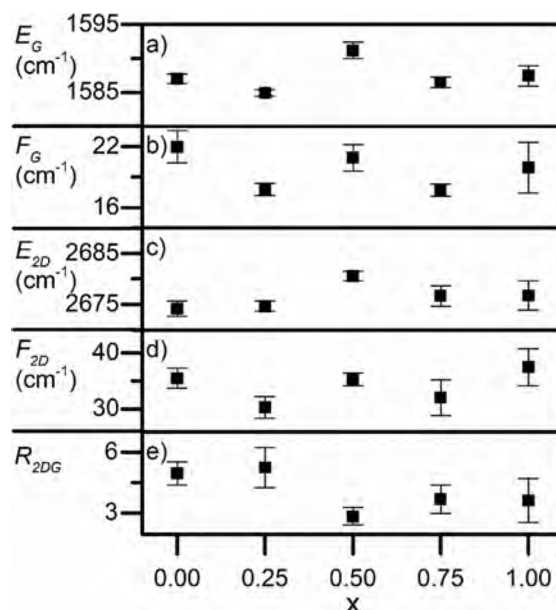

Fig. 5. Average values of: (a) E_G, (b) F_G, (c) E_{2D}, (d) F_{2D}, and (e) R_{2DG} for different NW compositions.

vanishes exponentially. This depends on the electric field and the broadening energy [17]. In each sample, two signals were observed (Fig. 3). One, at a wavelength of approximately 360 nm, corresponded to the energy gap of GaN (marked by the brown line). The second line corresponded to the reflectivity from the AlGaN cap (marked by the green arrows). This reflectivity changed its position from approximately 355 nm for 3% of aluminium content, to approximately 330 nm for 15% of aluminium content. Both signals show a shape characteristic for the low electric field limit and no sign of Franz-Keldysh oscillations. Therefore, we can conclude that for low aluminium content, the polarisation charges are screened by the free carriers and there is no electric field in the AlGaN caps. This result casts doubt on whether the NW structure indeed reduces polarisation charge screening as was reported in the literature [14].

To trace the real influence of NW substrates, graphene Raman spectroscopy was performed. The representative Raman spectra of graphene on NWs are presented in Fig. 4a. Intensities of graphene bands in each sample are enhanced in contrast to the reference sample of graphene on the GaN epilayer. Enhancement factors for D and D’ bands in Al0 samples are significantly higher than those in the rest of the samples; however, analysis of the enhancement factors for each band shows no explicit correlation with the aluminium content (Fig. 4b).

To trace how the NW substrate affects graphene strain and carrier concentration, a statistical analysis of G and 2D band parameters, i.e., energies (E_G, E_{2D}), full width at half maximum (F_G, F_{2D}), and their intensity ratio (R_{2DG}), was performed. [18,19] No explicit correlation for any of these parameters with x was observed (Fig. 5a–e). This suggests that the graphene deposited on the NWs with similar density distribution is strained in a similar way, and aluminium content in the AlGaN caps does not significantly impact average carrier concentration in graphene. In order to measure with nanometre resolution the effects of different NW substrates on the carrier concentration, KPFM was applied. Local graphene self-induced nanogating by the NW substrate was previously reported [9]. Topography images confirmed low roughness of the graphene surface observed in SEM images (Fig. 6a–f). Spatial modulation of potential in the whole investigated samples was observed on the measured surface (Fig. 6f–j). Analysis of potential profiles (Fig. 6k–o) enabled us to estimate the value of potential modulation in graphene on axial heterostructure NWs. The average value of nanowire-induced potential modulation in graphene (ΔV) varied from 0.8 mV for the Al0 sample to 3.7 mV for the Al100 sample. For samples Al25-Al75 this parameter was equal to 3.4 mV, 3.4 mV, and 2.8 mV, respectively. Therefore, no explicit correlation between aluminium content and the value of potential modulation (ΔV) and the average value of potential ($\langle V \rangle$) was observed. Thus, KPFM results confirm the Raman spectroscopy results in which aluminium content generally does not affect the carrier concentration in graphene.

Experimental results show a screening of polarisation charges in NW structures, thus questioning the electromagnetic mechanism of enhancement and suggesting the chemical one. In order to confirm this, numerical simulations were applied. Calculations performed by the finite difference time domain method show the presence of electric field enhancement in the structure of randomly distributed NWs (Fig. 7a). However, the value of enhancement is lower than that observed in typical metallic plasmonic structures. Furthermore, our calculations show the absence of plasmonic absorption in the investigated spectral range. They suggest that the calculated enhancement can be caused by light interference (Fig. 7b). However, the interference effect was excluded in our previous results since the laser line is in the minimum of interference and the intensity ratios of the individual Raman band do not follow the interference spectrum (Fig. 4b) [9]. This discrepancy can be understood by taking into account that the simulation was performed on randomly distributed NWs of equal height, while on SEM images it can be seen that the real roughness of the NW substrate is low but still visible. Therefore, experimental results and numerical simulations show that the electromagnetic mechanism is not responsible for the SERS effect in graphene on NWs and suggest the occurrence of a chemical mechanism. Detection of possible chemical bonds or intermediary states between graphene and GaN NWs requires further experimental studies using X-ray photoelectron spectroscopy and scanning tunnelling spectroscopy.

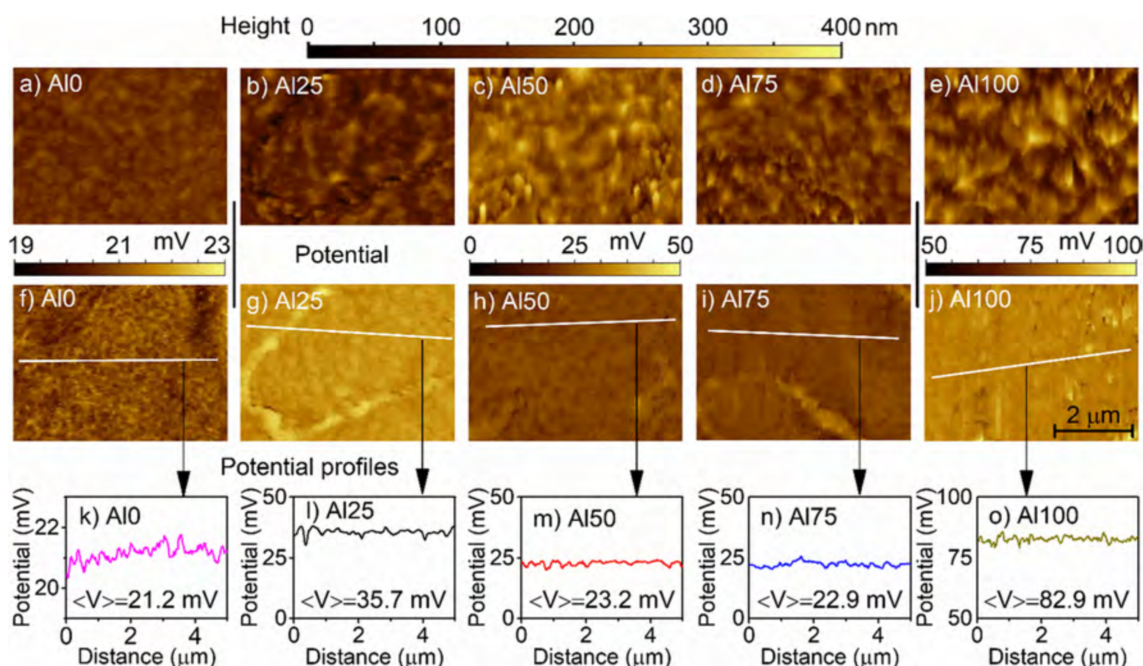

Fig. 6. KPFM images of the topography of the investigated samples (a–e), potential distribution (f–j), and representative potential profiles (k–o).

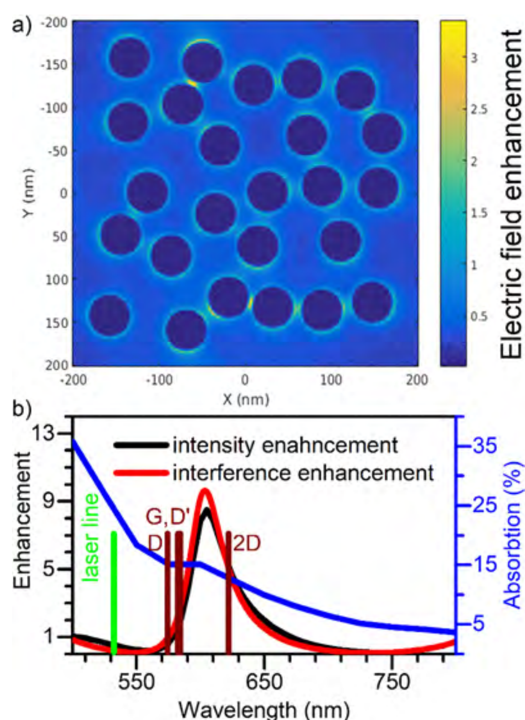

Fig. 7. (a) 2D map of electric field enhancement in graphene deposited on GaN NWs, (b) dependence of electric field enhancement, absorption and interference intensity enhancement on wavelength.

4. Conclusions

We observed the surface-enhanced Raman scattering effect in graphene deposited on AlGaN NWs with different aluminium contents. We calculated the value of total polarisation in AlGaN and found out that the value of sheet polarisation charge concentration on the top of the NWs is correlated with Al content. Interestingly, different amounts of Al do not affect the enhancement factors of the graphene Raman bands. The detailed analysis of Raman bands showed the presence of screening of polarisation charges. This was confirmed by KPFM and electroreflectance results. Therefore, experimental results question the possibility of the electromagnetic mechanism being responsible for the observed SERS. Additionally, numerical calculations also excluded the electromagnetic mechanism of the observed enhancement of the graphene Raman spectra. Therefore, our results suggest a chemical mechanism to be responsible for the observed enhancement.

Acknowledgements

This work was partially supported by the Ministry of Science and Higher Education in years 2015–2019 as a research grant “Diamond Grant” (No. DI2014 015744).” Financial support from the Polish Nacional Science Centre under grants 2016/21/N/ST3/03381 and 2016/23/B/ST7/03745 as well as by the European Union within European Regional Development Fund, grant POIG.01.03.01-00-159/08 (InTechFun) is acknowledged. This work was supported by the Research Foundation Flanders (FWO) under Grant no. EOS 30467715.

Appendix A. Supplementary material

Supplementary data to this article can be found online at https://doi.org/10.1016/j.apsusc.2019.01.040.

References

[1] G. Fan, H. Zhu, K. Wang, J. Wei, X. Li, Q. Shu, N. Guo, D. Wu, Graphene/silicon nanowire schottky junction for enhanced light harvesting, ACS Appl. Mater. Interfaces 3 (2011) 721–725, https://doi.org/10.1021/am1010354.

[2] H. Park, S. Chang, X. Zhou, J. Kong, T. Palacios, S. Gradečak, Flexible graphene electrode-based organic photovoltaics with record-high efficiency, Nano Lett. 14 (2014) 5148–5154, https://doi.org/10.1021/nl501981f.

[3] A.V. Babichev, H. Zhang, P. Lavenus, F.H. Julien, A.Y. Egorov, Y.T. Lin, L.W. Tu, M. Tchernycheva, GaN nanowire ultraviolet photodetector with a graphene transparent contact, Appl. Phys. Lett. 103 (2013) 201103, https://doi.org/10.1063/1.4829756.

[4] D.-W. Jeon, W.M. Choi, H.-J. Shin, S.-M. Yoon, J.-Y. Choi, L.-W. Jang, I.-H. Lee, Nanopillar InGaN/GaN light emitting diodes integrated with homogeneous multilayer graphene electrodes, J. Mater. Chem. 21 (2011) 17688, https://doi.org/10.1039/c1jm13640b.

[5] M. Tchernycheva, P. Lavenus, H. Zhang, A.V. Babichev, G. Jacopin, M. Shahmohammadi, F.H. Julien, R. Ciechonski, G. Vescovi, O. Kryliouk, InGaN/GaN core-shell single nanowire light emitting diodes with graphene-based P-

contact, Nano Lett. 14 (2014) 2456–2465, https://doi.org/10.1021/nl5001295.

[6] H. Bae, H. Rho, J.W. Min, Y.T. Lee, S.H. Lee, K. Fujii, H.J. Lee, J.S. Ha, Improvement of efficiency in graphene/gallium nitride nanowire on Silicon photoelectrode for overall water splitting, Appl. Surf. Sci. 422 (2017) 354–358, https://doi.org/10.1016/j.apsusc.2017.05.215.

[7] J. Kierdaszuk, P. Kaźmierczak, A. Drabińska, K. Korona, A. Wołoś, M. Kamińska, A. Wysmołek, I. Pasternak, A. Krajewska, K. Pakuła, Z.R. Zytkiewicz, Enhanced Raman scattering and weak localization in graphene deposited on GaN nanowires, Phys. Rev. B. 92 (2015) 195403, https://doi.org/10.1103/PhysRevB.92.195403.

[8] S. Shivaraman, R.A. Barton, X. Yu, J. Alden, L. Herman, M. Chandrashekhar, J. Park, P.L. McEuen, J.M. Parpia, H.G. Craighead, M.G. Spencer, Free-standing epitaxial graphene, Nano Lett. 9 (2009) 3100–3105, https://doi.org/10.1021/nl900479g.

[9] J. Kierdaszuk, P. Kaźmierczak, R. Bożek, J. Grzonka, A. Krajewska, Z.R. Zytkiewicz, M. Sobanska, K. Klosek, A. Wołoś, M. Kamińska, A. Wysmołek, A. Drabińska, Surface-enhanced Raman scattering of graphene caused by self-induced nanogating by GaN nanowire array, Carbon N. Y. 128 (2018) 70–77, https://doi.org/10.1016/j.carbon.2017.11.061.

[10] C. Muehlethaler, A. Odate, J.L. Weyher, I. Dzięcielewski, J.R. Lombardi, Enhanced Raman spectra of black dye N719 on GaN nanowires, Appl. Surf. Sci. 457 (2018) 809–814, https://doi.org/10.1016/j.apsusc.2018.06.276.

[11] S. Nie, S. Emory, Probing single molecules and single nanoparticles by surface-enhanced Raman scattering, Science 275 (1997) 1102–1106, https://doi.org/10.1126/science.275.5303.1102.

[12] O. Ambacher, J. Smart, J.R. Shealy, N.G. Weimann, K. Chu, M. Murphy, W.J. Schaff, L.F. Eastman, R. Dimitrov, L. Wittmer, M. Stutzmann, W. Rieger, J. Hilsenbeck, Two-dimensional electron gases induced by spontaneous and piezoelectric polarization charges in N- and Ga-face AlGaN/GaN heterostructures, J. Appl. Phys. 85 (1999) 3222–3233, https://doi.org/10.1063/1.369664.

[13] T. Takeuchi, C. Wetzel, S. Yamaguchi, H. Sakai, H. Amano, I. Akasaki, Y. Kaneko, S. Nakagawa, Y. Yamaoka, N. Yamada, Determination of piezoelectric fields in strained GaInN quantum wells using the quantum-confined Stark effect, Appl. Phys. Lett. 73 (1998) 1691–1693, https://doi.org/10.1063/1.122247.

[14] N. Jamond, P. Chrétien, F. Houzé, L. Lu, L. Largeau, O. Maugain, L. Travers, J.C. Harmand, F. Glas, E. Lefeuvre, M. Tchernycheva, N. Gogneau, Piezo-generator integrating a vertical array of GaN nanowires, Nanotechnology. 27 (2016) 325403, https://doi.org/10.1088/0957-4484/27/32/325403.

[15] S.R. Kurtz, A.A. Allerman, D.D. Koleske, G.M. Peake, Electroreflectance of the AlGaN/GaN heterostructure and two-dimensional electron gas, Appl. Phys. Lett. 80 (2002) 4549–4551, https://doi.org/10.1063/1.1487447.

[16] A. Drabińska, Photo- and Electroreflectance Spectroscopy of Low-Dimensional III-Nitride Structures, Acta Phys. Pol. A 104 (2003) 149–164, https://doi.org/10.12693/APhysPolA.104.149.

[17] D.E. Aspnes, Band nonparabolicities, broadening, and internal field distributions: the spectroscopy of Franz-Keldysh oscillations, Phys. Rev. B. 10 (1974) 4228–4238, https://doi.org/10.1103/PhysRevB.10.4228.

[18] A. Das, S. Pisana, B. Chakraborty, S. Piscanec, S.K. Saha, U.V. Waghmare, K.S. Novoselov, H.R. Krishnamurthy, A.K. Geim, A.C. Ferrari, A.K. Sood, Monitoring dopants by Raman scattering in an electrochemically top-gated graphene transistor, Nat. Nanotechnol. 3 (2008) 210–215, https://doi.org/10.1038/nnano.2008.67.

[19] T.M.G. Mohiuddin, A. Lombardo, R.R. Nair, A. Bonetti, G. Savini, R. Jalil, N. Bonini, D.M. Basko, C. Galiotis, N. Marzari, K.S. Novoselov, A.K. Geim, A.C. Ferrari, Uniaxial strain in graphene by Raman spectroscopy: G peak splitting, Grüneisen parameters, and sample orientation, Phys. Rev. B - Condens. Matter Mater. Phys. 79 (2009) 205433, https://doi.org/10.1103/PhysRevB.79.205433.

[20] A. Reserbat-Plantey, D. Kalita, L. Ferlazzo, S. Autier-Laurent, K. Komatsu, C. Li, R. Weil, Z. Han, A. Ralko, L. Marty, S. Guéron, N. Bendiab, H. Bouchiat, V. Bouchiat, Strain superlattices and macroscale suspension of Graphene induced by corrugated substrates, Nano Lett. 14 (2014) 5044–5051, https://doi.org/10.1021/nl5016552.

[21] H. Mi, S. Mikael, C.-C. Liu, J.-H. Seo, G. Gui, A.L. Ma, P.F. Nealey, Z. Ma, Creating periodic local strain in monolayer graphene with nanopillars patterned by self-assembled block copolymer, Appl. Phys. Lett. 107 (2015) 143107, , https://doi.org/10.1063/1.4932657.

[22] M. Nonnenmacher, M.P. O'Boyle, H.K. Wickramasinghe, Kelvin probe force microscopy, Appl. Phys. Lett. 58 (1991) 2921–2923, https://doi.org/10.1063/1.105227.

[23] A. Wierzbicka, Z.R. Zytkiewicz, S. Kret, J. Borysiuk, P. Dluzewski, M. Sobanska, K. Klosek, A. Reszka, G. Tchutchulashvili, A. Cabaj, E. Lusakowska, Influence of substrate nitridation temperature on epitaxial alignment of GaN nanowires to Si (111) substrate, Nanotechnology 24 (2013) 035703, https://doi.org/10.1088/0957-4484/24/3/035703.

[24] T. Ciuk, I. Pasternak, A. Krajewska, J. Sobieski, P. Caban, J. Szmidt, W. Strupinski, Properties of chemical vapor deposition graphene transferred by high-speed electrochemical delamination, J. Phys. Chem. C 117 (2013) 20833–20837, https://doi.org/10.1021/jp4032139.

[25] I. Pasternak, A. Krajewska, K. Grodecki, I. Jozwik-Biala, K. Sobczak, W. Strupinski, Graphene films transfer using marker-frame method, AIP Adv. 4 (2014) 097133, https://doi.org/10.1063/1.4896411.

[26] A. Pierret, C. Bougerol, S. Murcia-Mascaros, A. Cros, H. Renevier, B. Gayral, B. Daudin, Growth, structural and optical properties of AlGaN nanowires in the whole composition range, Nanotechnology 24 (2013) 115704, https://doi.org/10.1088/0957-4484/24/11/115704.

[27] R.F. Allah, T. Ben, R. Songmuang, D. González, Imaging and analysis by transmission electron microscopy of the spontaneous formation of Al-rich shell structure in Al$_{x}$Ga$_{1-x}$N/GaN nanowires, Appl. Phys Express 5 (2012) 045002, https://doi.org/10.1143/APEX.5.045002.

[28] A. Reszka, A. Wierzbicka, K. Sobczak, U. Jahn, U. Zeimer, A.V. Kuchuk, A. Pieniążek, M. Sobanska, K. Klosek, Z.R. Zytkiewicz, B.J. Kowalski, An influence of the local strain on cathodoluminescence of GaN/Al x Ga 1–x N nanowire structures, J. Appl. Phys. 120 (2016) 194304, https://doi.org/10.1063/1.4968004.